

# Microhardness and structure of thick silica films prepared by vacuum deposition

K. AIKAWA, H. SAKATA, S. FURUUCHI

*Research Laboratory, Asahi Glass Co. Ltd., Yokohama 221, Japan*

The relationships are investigated between the microhardness, density and composition of silica films 7 to 10  $\mu\text{m}$  thick prepared by resistance heating and electron beam evaporation. The Vickers hardness of the film prepared by electron beam evaporation gives 180 to 620  $\text{kg mm}^{-2}$  for varying pressures and is higher than that of film prepared by resistance heating evaporation. The silica films of higher density show higher hardness irrespective of the kinds of evaporation. The porosity of the films, which is 0 to 30% and decreases with lowering pressure, is estimated from the ratio of measured density of the film to assumed bulk density.

## 1. Introduction

There have been few papers on the hardness of vacuum evaporated thin films because of the difficulty of measuring their genuine hardness. Palatnik and Gladkikh [1] investigated the microhardness and microstructure of metal films (thickness: 20 to 300  $\mu\text{m}$ ) deposited in vacuum. Nishibori and Kinoshita [2] recently studied the hardness of  $\text{MgF}_2$  and  $\text{LiF}$  films 0.1 to 1  $\mu\text{m}$  thick, using their constructed Vickers type ultra-microhardness tester. Further, hardness of  $\text{TiC}$  films made by activated reactive evaporation from 6 to 125  $\mu\text{m}$  in thickness were measured by Bunshah and Raghuram [3, 4].

Evaporated silica films are used for protective films for surface mirrors and plastics, optical thin films [5, 6] insulating films for thin film devices [7]. Although optical and dielectrical properties of silica films have been widely studied, the hardness of these films in relation to their structure has not been well established. In fact, stoichiometry of evaporated silica films can be varied by film preparation conditions, e.g. pressure and deposition rate [8].

In the present work, we investigated the hardness of vacuum-deposited silica protective films. This paper describes the relationships between the microhardness, density and composition of thick silica films prepared by resistance heating or by electron beam evaporation, and these properties

are examined as a function of pressure in film preparation.

## 2. Experimental

### 2.1. Sample preparation

Silicon monoxide ( $\text{SiO}$ ) and fused quartz ( $\text{SiO}_2$ ) were used as evaporants in the case of resistance heating (RH) and electron beam (EB) evaporation, respectively. The films were deposited on commercial glass substrates at pressures ranging from  $1 \times 10^{-3}$  to  $5 \times 10^{-5}$  torr, where the distance from the source to the substrate was 17 cm for the two evaporation methods. The rate of deposition was  $1 \mu\text{m min}^{-1}$  for RH and  $0.5 \mu\text{m min}^{-1}$  for EB evaporation.

The evaporated silica films over 7  $\mu\text{m}$  in thickness [9] were used for measurement of hardness and density, and the films less than 2  $\mu\text{m}$  thick were used for identifying their composition.

### 2.2. Film hardness, density and composition

The Vickers microhardness was measured, eliminating the effect of glass substrate, under a load of 25 g for a loading time of 30 sec. The hardness value was determined as the average from 10 measurements for each specimen.

The density of the evaporated silica films was determined by measuring its mass, area and thickness. The mass was measured after the specimen

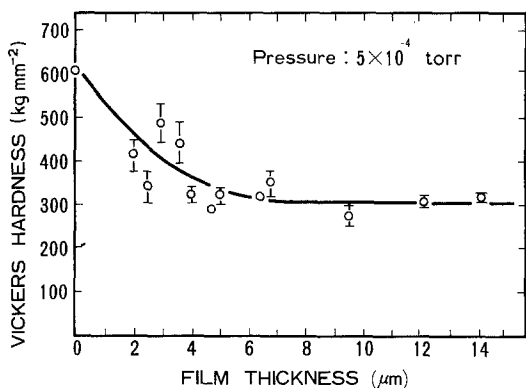


Figure 1 Vickers microhardness versus thickness of silica films evaporated on glass substrate by electron beam evaporation.

had been kept in a desiccator for 1 h after deposition to avoid water absorption into the film.

Since infrared spectroscopy is a useful method for identifying silicon oxides [8], we examined the infrared absorption spectra of the silica films deposited on KBr plates at various pressures.

### 3. Results

#### 3.1. Film thickness and hardness

Preliminary experiments were made to find a minimum thickness of silica films necessary for eliminating the effect of substrate on the film hardness. The microhardness was measured for films of varying thickness prepared on the glass substrate by EB evaporation at  $5 \times 10^{-4}$  torr. Fig. 1 shows the results of the hardness measurements as a function of film thickness, where the open circles and bars indicate the average and scattering range of 10 measurements for each specimen. The hardness is seen to decrease with an increase of film thickness up to  $6 \mu\text{m}$ , and then to stay constant at about  $300 \text{ kg mm}^{-2}$  for film thicknesses over  $7 \mu\text{m}$ . Since the depth of the indenter into the film is calculated from the diamond pyramid impression to be  $2.5 \mu\text{m}$  and this depth is less than the film thickness ( $\sim 7 \mu\text{m}$ ), the constant hardness value gives the genuine hardness ( $300 \text{ kg mm}^{-2}$ ) of the film. The higher hardness values of the films with thickness smaller than  $6 \mu\text{m}$  reflects the effect of the glass substrate, the Vickers hardness of which was measured to be  $610 \text{ kg mm}^{-2}$ . Accordingly, in subsequent microhardness measurements we used the films of the order of  $10 \mu\text{m}$  in thickness so that the effect of the substrate could be eliminated.

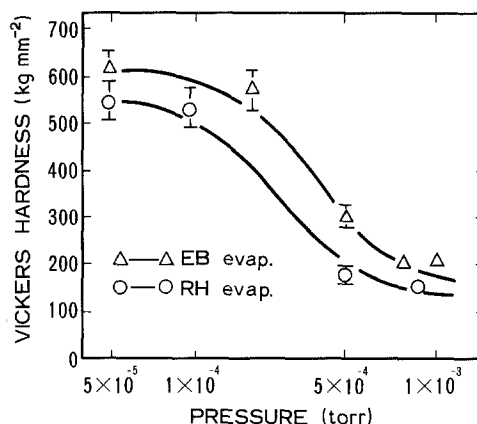


Figure 2 Variation of hardness for silica films deposited by electron beam and resistance heating evaporation as functions of pressure.

#### 3.2. Pressure and film hardness

The variation of film hardness in relation to environmental pressure during film deposition is shown in Fig. 2 for two kinds of films, i.e. those obtained by RH and EB evaporation. The hardness of the films prepared by both evaporating methods at  $1 \times 10^{-3}$  to  $5 \times 10^{-5}$  torr was found to be  $150$  to  $620 \text{ kg mm}^{-2}$ . As Fig. 2 shows, the highest film hardness,  $620 \text{ kg mm}^{-2}$ , was obtainable at  $5 \times 10^{-5}$  torr by EB evaporation, which was almost the same hardness value as that observed for commercial glass plate ( $610 \text{ kg mm}^{-2}$ ) but was less than that of fused quartz ( $720 \text{ kg mm}^{-2}$ ).

#### 3.3. Pressure and film density

Fig. 3 shows the relation between the film density and pressures during deposition. The density of the film made by EB evaporation at  $5 \times 10^{-5}$  torr was determined to be about  $2.02 \text{ g cm}^{-3}$  which

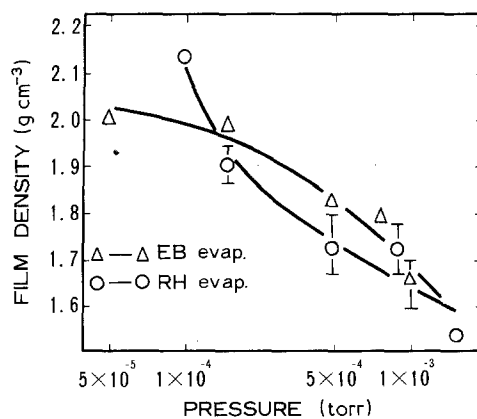


Figure 3 Film density versus pressure.

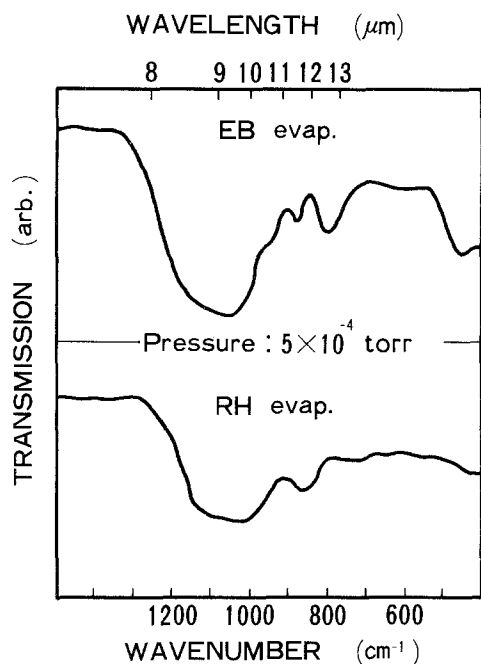


Figure 4 Infrared transmission spectra of vacuum-deposited silica films.

was less than that of fused quartz at  $2.20 \text{ g cm}^{-3}$ , while that of the films by RH evaporation at  $1 \times 10^{-4}$  torr was about  $2.13 \text{ g cm}^{-3}$ , which was slightly less than that of silicon monoxide ( $2.15 \pm 0.03 \text{ g cm}^{-3}$ ) [10].

### 3.4. Pressure and film composition

Figs. 4 and 5 show the infrared absorption spectra of the silica films prepared by RH and EB evaporation at  $5 \times 10^{-4}$  and  $5 \times 10^{-5}$  torr. It was found that composition of the silica films differed depending upon the kinds of evaporants and evaporation methods even at the same pressure.

A moderate absorption band near  $11.4 \mu\text{m}$  together with a strong absorption band at  $9.6 \mu\text{m}$ , identifiable as  $\text{Si}_2\text{O}_3$ , was found for the film evaporated by RH evaporation [8]. On the other hand, the EB evaporated film showed a strong band at  $9.2 \mu\text{m}$  and moderate ones at  $12.5$  and  $11.4 \mu\text{m}$ , which means that this film consists of a mixture of  $\text{SiO}_2$  and  $\text{Si}_2\text{O}_3$ .

In evaporating at  $5 \times 10^{-5}$  torr, the spectrum of the film prepared by RH evaporation showed a strong absorption band at  $10 \mu\text{m}$ , identifiable as  $\text{SiO}$ . The EB evaporated film gave a strong absorption at  $9.2 \mu\text{m}$  and an absorption at  $12.5 \mu\text{m}$ , the same spectrum as  $\text{SiO}_2$ . As described already, the amount of oxygen combined with vaporized Si

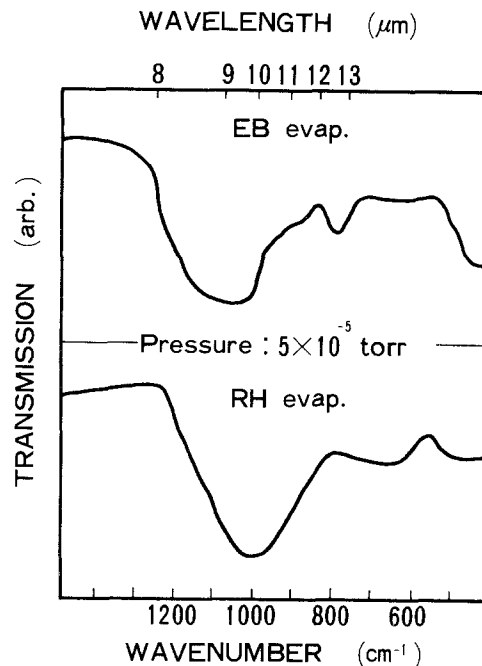


Figure 5 Infrared transmission spectra of vacuum-deposited silica films.

was dependent on oxygen partial pressure during deposition. The results of the analysis are summarized in Fig. 6 as relations between pressure and film composition. Furthermore, combining with the measurements of film density, the following was concluded: for the films prepared by RH evaporation, the film ranging from about  $1.83$  to  $2.13 \text{ g cm}^{-3}$  in density is  $\text{Si}_2\text{O}_3$ ; of the films prepared by EB evaporation, the film over  $2.0 \text{ g cm}^{-3}$  in density is  $\text{SiO}_2$  and that from about  $1.65$  to  $2.0 \text{ g cm}^{-3}$  is a mixture of  $\text{SiO}_2$  and  $\text{Si}_2\text{O}_3$ .

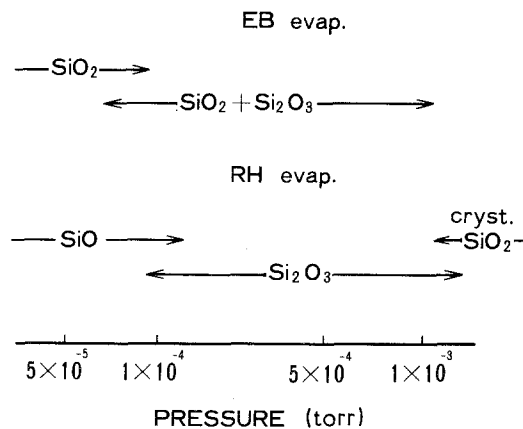


Figure 6 Composition of silica films versus pressure during evaporation.

## 4. Discussion

### 4.1. Pressure and film hardness

The highest hardness value obtained was nearly equal to that of commercial glass plate, but less than that of fused quartz (see Section 3.2). The hardness of the polished surface of a fused quartz bulk specimen, a pure amorphous  $\text{SiO}_2$ , was found to be about  $750 \text{ kg mm}^{-2}$ . As shown in Fig. 2, the highest hardness observed for the EB evaporated silica films having  $\text{SiO}_2$  structure is  $620 \text{ kg mm}^{-2}$ , which is about four-fifths that of fused quartz. This may be ascribed to the porous character of evaporated silica films considering the result of film density in Fig. 3.

The hardness and density of the films made by RH and EB evaporation decreased gradually with increasing pressure (Figs. 2 and 3). This may be because the mean free path of vapour molecules becomes shorter with increasing pressure, and that the collision probability of vapour molecules with residual gas molecules increases. This process would produce a loose film containing many pores which can adsorb water, oxygen or nitrogen gases, and finally results in the density lowering of the film.

The hardness of silica films by EB evaporation was higher than that of the films by RH evaporation and this hardness difference was larger for lower pressures. To discuss this, we consider first that the difference of composition of the silica film depends upon the evaporation methods; the film by EB evaporation at  $\sim 10 \times 10^{-5}$  torr was  $\text{SiO}_2$  and that by RH evaporation was  $\text{SiO}$ . Also the EB-deposited film consisted of a mixture of  $\text{SiO}_2$  and  $\text{Si}_2\text{O}_3$  and the film made by RH evaporation was  $\text{Si}_2\text{O}_3$  at 1 to  $10 \times 10^{-4}$  torr. Secondly, the density of the silica films by EB evaporation was relatively higher than that of the films by RH evaporation, as shown in Fig. 3. Although the density of the silica films by RH evaporation was higher than that of the films by EB evaporation under  $2 \times 10^{-4}$  torr in pressure (Fig. 3), it does not contradict the results in Fig. 8 that the hardness of the film by EB evaporation is higher than that by RH evaporation with the same density.

### 4.2. Pressure and film density

The density of the films decreased with increasing pressure as shown in Fig. 3; this suggests that the film contains many micro-pores in itself as described in Section 4.1. The film density was found to be about  $1.6 \text{ g cm}^{-3}$ , being independent of the

evaporation methods at  $2 \times 10^{-3}$  torr, while the films by EB evaporation showed a higher density than that of the films by RH evaporation at 2 to  $10 \times 10^{-4}$  torr. From the analysis of the infrared absorption spectra (see Section 3.4), the EB evaporated film was identified as a mixture of  $\text{SiO}_2$  and  $\text{Si}_2\text{O}_3$  and the film by RH to be  $\text{Si}_2\text{O}_3$  at 1 to  $10 \times 10^{-4}$  torr. As a result the former film has a slightly higher density than the latter one because it contains  $\text{SiO}_2$ . Although the RH evaporated film at  $1 \times 10^{-4}$  torr was identified to be of  $\text{SiO}$  composition and the film density to be nearly the same as the bulk density of  $\text{SiO}$ , it is actually supposed that the film contains pure silicon whose bulk density is  $2.40 \text{ g cm}^{-3}$  [11] and higher than that of  $\text{SiO}$  ( $2.15 \text{ g cm}^{-3}$ ).

The porosity of the film can be expressed as the ratio of true density of the film material to the measured film density. Accordingly, assuming the true density, we estimate the porosity of the films using the data in Fig. 3, as a function of environmental pressure during film deposition. Pliskin *et al.* [8], described  $\text{Si}_2\text{O}_3$  as an intermediate oxide between  $\text{SiO}$  and  $\text{SiO}_2$ , but Namba *et al.* [12] reported that  $\text{SiO}$  film consisted a mixture of  $\text{Si}$  and  $\text{SiO}_2$ . For  $\text{SiO}_x$  film prepared by us we can not determine an accurate value of  $x$  for the film from only the infrared absorption spectra of the film, so that more detailed study is needed to examine stoichiometry of the films. We assume here the density of  $\text{Si}_2\text{O}_3$  to be  $2.175 \text{ g cm}^{-3}$ , which is an average of bulk density of  $\text{SiO}$  ( $2.15 \text{ g cm}^{-3}$ ) and  $\text{SiO}_2$  ( $2.20 \text{ g cm}^{-3}$ ). In the same manner the density of the mixture of  $\text{SiO}_2$  and  $\text{Si}_2\text{O}_3$  in ratio 1:1 is assumed to be  $2.188 \text{ g cm}^{-3}$ . For the  $\text{Si}_2\text{O}_3$  film, even if the density ratio of  $\text{SiO}_2$  to  $\text{SiO}$  varies from 1:0 to 0:1, that density  $\rho_{\text{Si}_2\text{O}_3}$  lies between  $2.15 \text{ g cm}^{-3}$  ( $\rho_{\text{SiO}}$ ) and  $2.20 \text{ g cm}^{-3}$  ( $\rho_{\text{SiO}_2}$ ). That is, the difference ( $\rho_{\text{SiO}_2} - \rho_{\text{SiO}}$ ) is at the most  $0.05 \text{ g cm}^{-3}$ , causing an error  $0.05 \text{ g cm}^{-3} / 2.175 \text{ g cm}^{-3} = 0.023$  in the assumed value  $\rho_{\text{Si}_2\text{O}_3} = 2.175 \text{ g cm}^{-3}$ . As this means a relative error of  $\pm 1.2\%$  in the calculated porosity, we consider the assumption of the ratio  $\text{SiO}$  to  $\text{Si}_2\text{O}_3$  1:1 to be moderate. For the mixed film of  $\text{SiO}_2$  and  $\text{Si}_2\text{O}_3$ , we assumed the density to be  $2.188 \text{ g cm}^{-3}$  ( $(\rho_{\text{SiO}_2} + \rho_{\text{Si}_2\text{O}_3})/2$ ). In this case, the difference ( $\rho_{\text{SiO}_2} - \rho_{\text{SiO}}$ ) is  $0.0125 \text{ g cm}^{-3}$ , which at most leads to a relative error of  $\pm 0.3\%$  in the porosity. Thus, we could calculate the bulk density of each film referring to the relation between pressure and film composition in Fig. 6 for

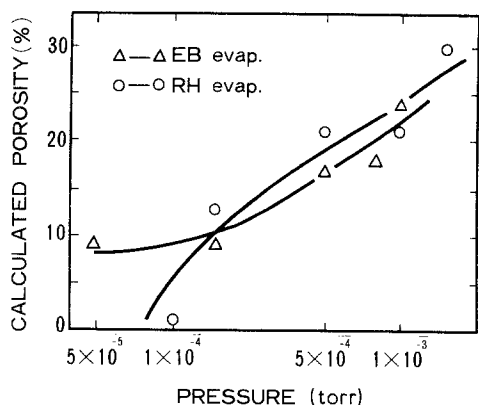


Figure 7 Calculated porosity of silica films versus pressure during film deposition.

both evaporation methods. The porosity of the film, i.e. the measured density of the film divided by density corresponding to the film composition, at any pressure could be deduced as shown in Fig. 7. Obviously the porosity rises with increasing pressure. In fact, we obtained a dense silica film having the porosity of nearly zero at  $1 \times 10^{-4}$  torr in RH evaporation and also a porous film with the porosity of about 10% in EB evaporation at a lower pressure of  $5 \times 10^{-5}$  torr. The porosity of the film by EB evaporation was more or less lower than that of the film by RH evaporation under  $2 \times 10^{-4}$  torr.

#### 4.3. Film density and hardness

The relation between the hardness and density of the silica film is shown in Fig. 8, by rearranging the experimental results. The silica films of higher density had higher hardness irrespective of the

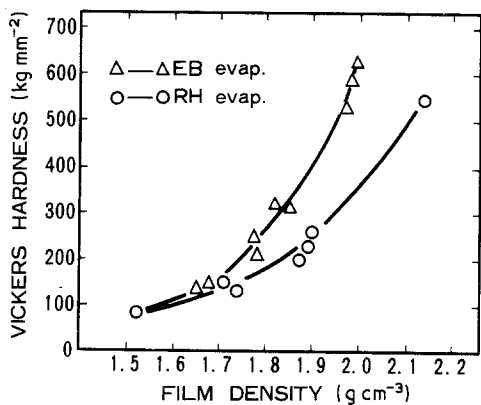


Figure 8 Relation between the density and the hardness of silica film prepared by resistance heating and electron beam evaporation at different pressures.

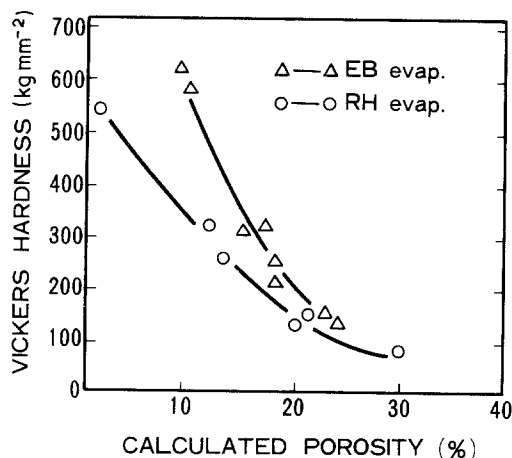


Figure 9 Vickers hardness versus calculated porosity.

evaporation methods. This result was considered to indicate the structure difference of two kinds of silica film, i.e. from the mixture of  $\text{SiO}_2$  and  $\text{Si}_2\text{O}_3$  to  $\text{SiO}_2$  for EB evaporation, and from  $\text{Si}_2\text{O}_3$  to  $\text{SiO}$  for RH evaporation, and further, the porosity decreases with increasing film density. Though the difference was negligibly small for the films of lower density, the hardness of the silica films obtained by EB evaporation was higher than that of the films by RH evaporation when the density was over  $1.75 \text{ g cm}^{-3}$ . This may be due to  $\text{Si}_2\text{O}_3$  film containing many pores by RH evaporation at higher pressures as shown in Fig. 7, resulting in lower hardness at the same evaporation conditions. Infrared spectroscopy made it clear that the silica film by EB evaporation was composed of a mixture of  $\text{SiO}_2$  and  $\text{Si}_2\text{O}_3$ . Following the procedure of estimating the porosity described in Section. 4.2, the porosity versus hardness of the silica films is given in Fig. 9. The film hardness decreases with increasing the porosity, and the film having the same porosity has a higher hardness in EB evaporation than in RH evaporation. These results suggest that fine structure of the pores in the film differs depending upon the means of preparing the film; however, on the other hand, considering that the process of film growth may not differ in each method of film preparation, it is a reasonable interpretation that the films have different compositions even when they have the same porosity.

#### References

1. L. S. PALATNIK and N. T. GLADKIKH, *Ind. Lab.* **30** (1964) 1355.
2. M. NISHIBORI and K. KINOSITA, *Japan. J. Appl. Phys.* **11** (1972) 758.

3. R. F. BUNSHAH and A. C. RAGHURAM, *J. Vac. Sci. Technol.* **9** (1972) 1385.
4. A. C. RAGHURAM and R. F. BUNSHAH, *ibid* **9** (1972) 1385.
5. G. HASS and C. D. SALZBERG, *J. Opt. Soc. Am.* **44** (1954) 181.
6. D. S. ALLAM and K. E. G. PITT, *Thin Solid Films* **1** (1967) 245.
7. D. R. POAT, *ibid* **4** (1969) 123.
8. W. A. PLISKIN and H. S. LEHMAN, *J. Electrochem. Soc.* **122** (1965) 1013.
9. S. FURUUCHI, H. SAKATA and K. AIKAWA, *Japan. J. Appl. Phys.* **13** (1974) 1905.
10. J. BENYON, *Vacuum* **20** (1970) 293.
11. G. HASS, *J. Amer. Ceram. Soc.* **33** (1950) 353.
12. A. KAWAZU, N. KANEKAWA and S. NAMBA, *Sci. Pap. Inst. Phys. Chem. Res.* **3** (1969) 63.

Received 7 January and accepted 2 May 1977.